

# Dynamics of the Central Andes: constraints from comprehensive observations of P-to-S converted phases

X. Yuan, S. V. Sobolev, R. Kind, O. Oncken, and Andes Seismology Group

GeoForschungsZentrum Potsdam, Freie Universitaet Berlin, University of Arizona & Universidad de Chile

Email: yuan@gfz-potsdam.de

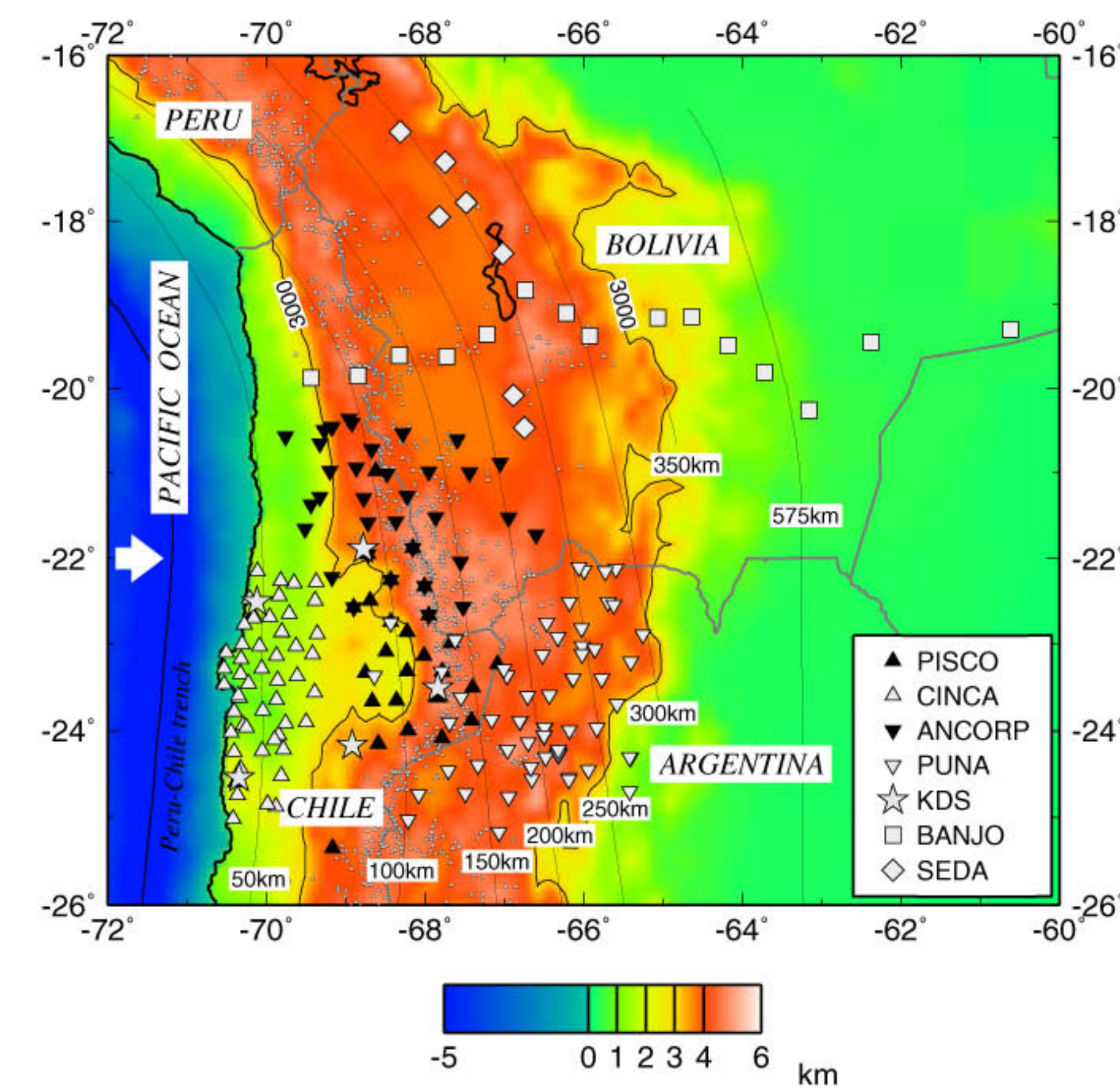
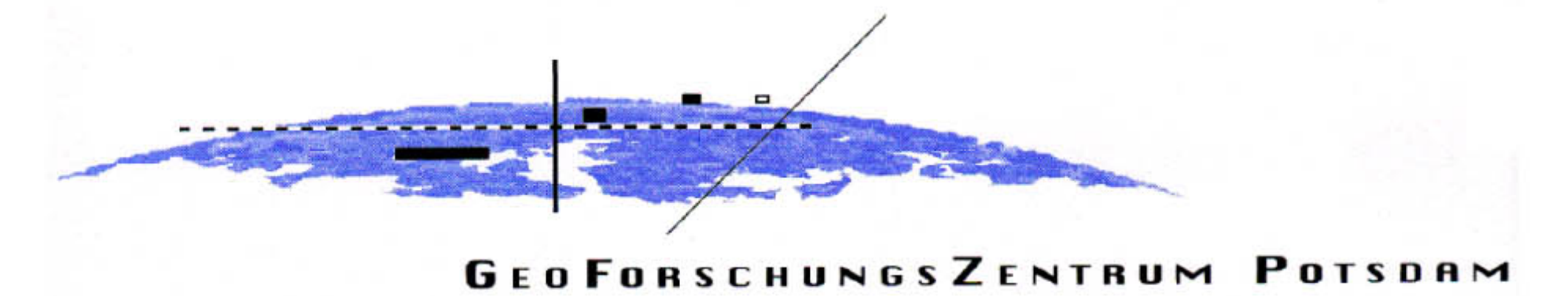
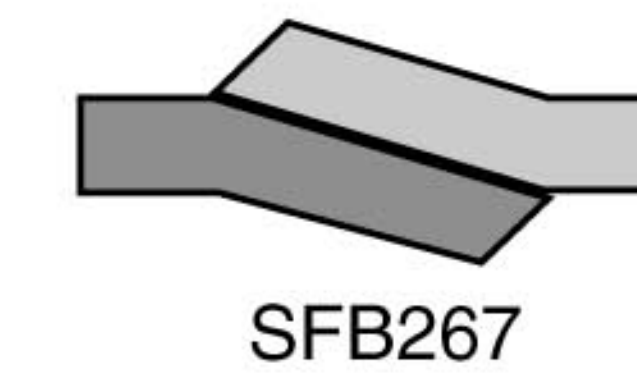


Fig. 1: Several temporal arrays of seismic stations were operated in northern Chile, southern Bolivia and northwestern Argentina for periods ranging from two months to one year supported by the Sonderforschungsbereich (SFB) 267 of the Deutsche Forschungsgemeinschaft and the US PASCALL project in cooperation with Chilean institutions. Most stations were equipped with short period 1 Hz Mark-L4 seismometers while a small number of stations were operated with broadband sensors (Guralp-3T and Streckeisen STS-2). The map shows these station arrays with different symbols. Small triangles are recent active volcanoes. Contour lines of Wadati-Benioff Zone are taken from Cahill and Isacks (1992).

We employ teleseismic P-to-S converted waves from temporary seismological networks operated in the Central Andes between 1994 and 1997 to image structures in the crust and upper mantle across the Andes. Several structural elements can be traced over hundreds of kilometers. The subducted oceanic crust is continuously seen to a depth of 120 km suggesting that gabbro is dynamically transported to that depth where it is completely converted to eclogite. Intermediate depth earthquakes tend to occur within the subducted oceanic crust and the immediately underlying lithospheric mantle. The continental Moho lies at 30 to 70 km depth correlating well with surface topography. The thickened crust beneath the plateau has a high  $V_p/V_s$  ratio of about 1.80, indicating large scale partial melting in the crust. In the continental upper plate, a west-dipping intracrustal low velocity zone more than 300 km long possibly marks the top of the upper crust of the Brazilian margin, which thus seems to be underthrust further west under the Altiplano than previously thought. The 660 km discontinuity is depressed by 30–40 km in the slab region indicated by high P velocity in the tomographic model, suggesting a temperature decrease of 300–500 K.

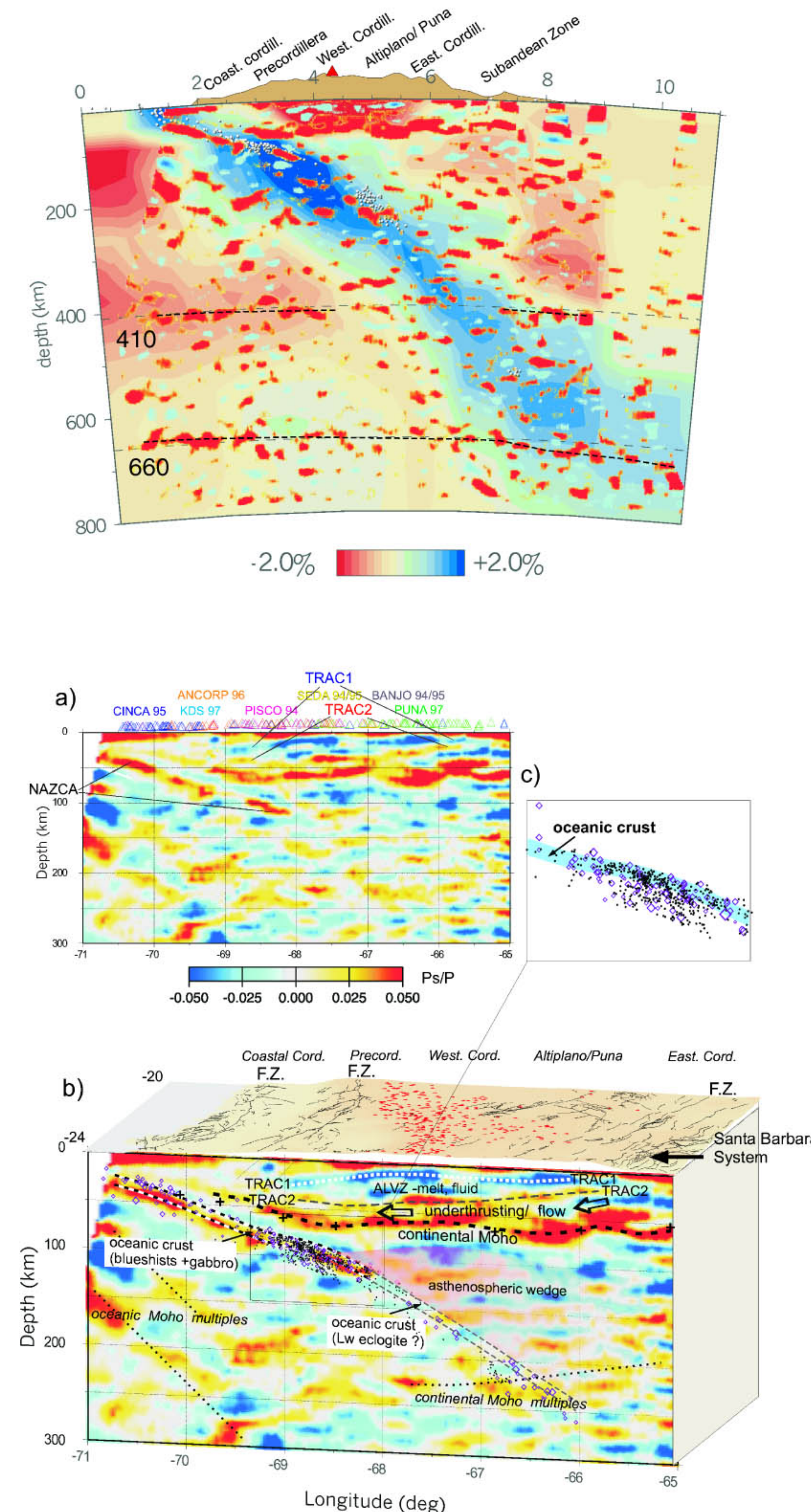


Fig. 3: Migrated receiver function image of the upper mantle in the Central Andes down to 800 km depth. IASP91 model corrected for the local changes of crustal velocity and thickness across the central Andes was used for the migration. Records from all stations are used. Red colors mark positive amplitudes of the receiver functions related to an increase of velocity downwards and blue colors mark negative amplitudes. Amplitudes are normalized. Receiver function image is compared with the P wave tomography (Bijwaard et al. 1999) shown in the background. The 410 km discontinuity is well observed in the west part of the profile, but not imaged in the vicinity of the slab indicated by high P velocity (blue color in tomographic model). The 660 km discontinuity is depressed by 30–40 km within the slab, implying a temperature reduction of 300–600° in the subducted Nazca plate.

Fig. 4: a) Zoom of the migrated receiver function image of the Central Andes in the region of the dense station distribution. True amplitude receiver function image is displayed. b) Black pluses show Moho depth data from wide-angle reflection studies (Wigger et al., 1994). TRAC1 and TRAC2 convertors bound the low velocity zone (ALVZ) which dips westwards from the Santa Barbara System in the Eastern Cordillera (faults are indicated by black lines at the surface) across the entire Altiplano/Puna to the Precordillera. The ALVZ is interpreted as a partial melted zone resulted from the underthrusting of the Brazilian shield margin under the entire Altiplano to the Precordillera. The Nazca convertor (thick black-white dashed line) is interpreted as an image of the oceanic Moho. Upper boundary of the oceanic crust (slab shear zone) is set 10 km above the oceanic Moho in agreement with the results of waveform modelling (Fig. 5). Oceanic crust is clearly visible from converted waves only down to 120 km depth. c) Zoom of the intermediate depth earthquake cluster. Black dots are earthquakes located by the PISCO network. Purple diamonds are 1965-1995 relocated events at 22–24°S, with the depth corrected for the local velocity model in the Central Andes. Blue domain is the oceanic crust from interpretation of the receiver function waveforms. Note that upper bound of the earthquake cluster matches nearly exactly the top of the oceanic crust. Most of the events are located within the oceanic crust, but the middle section of the cluster is extended below the oceanic crust by 20 km.

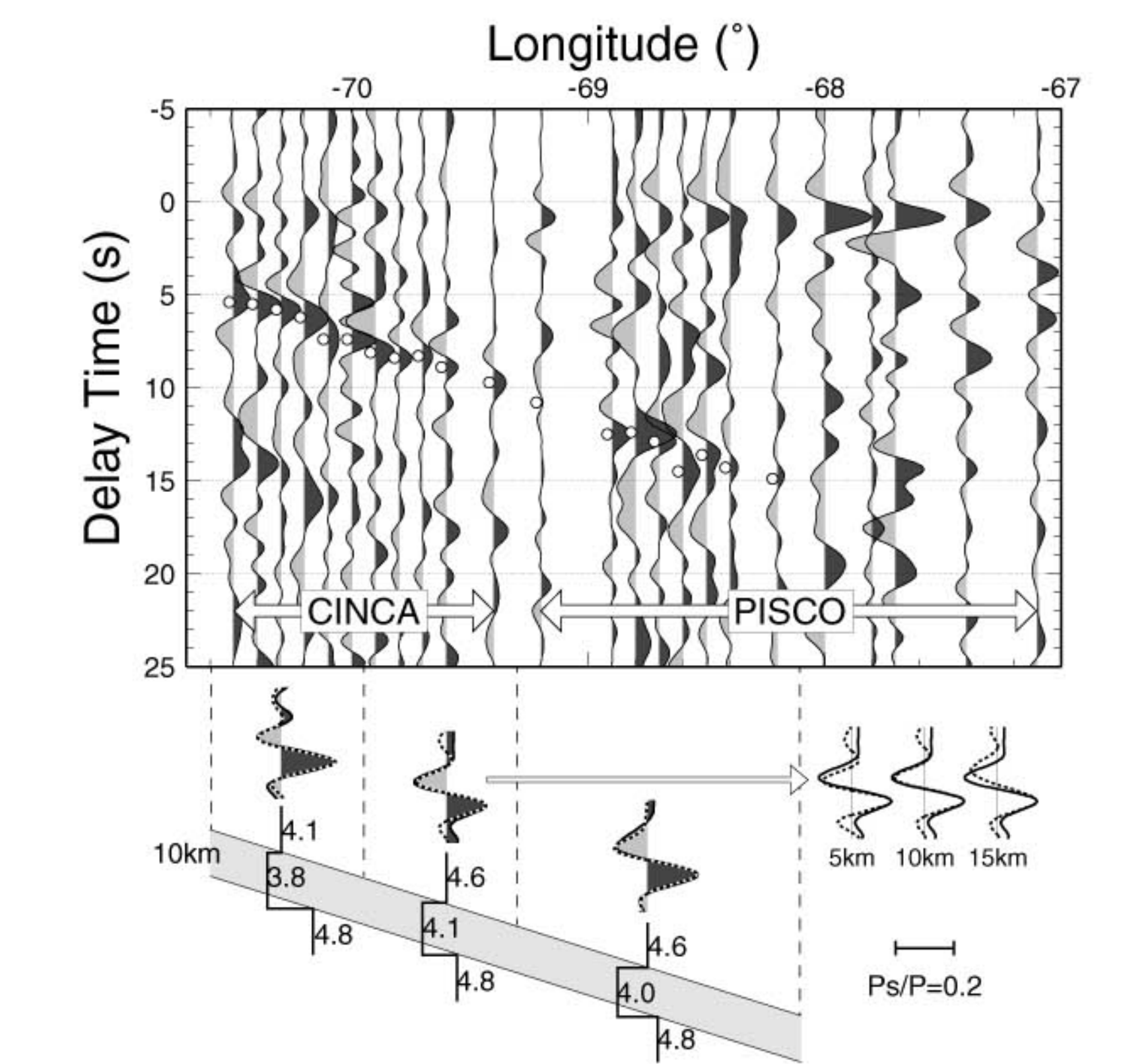


Fig. 5: Receiver functions from teleseismic earthquakes in South Sandwich Island recorded by CINCA network and from deep regional earthquakes in Argentina recorded by PISCO network are sorted from west to east by the geographic longitude of stations and stacked in bins of 5 km. A dipping P-to-S conversion phase can be clearly traced from 5 s to 15 s delay times. Positive amplitudes of the converted waves (black) are coherently followed by negative amplitudes (gray). Stacked receiver function waveforms can be modeled by a response of a 10 km thick layer with about 15% S velocity reduction relative to the surrounding mantle. The low velocity layer is interpreted as the subducted oceanic crust where basaltic rocks do not completely transform to eclogitic rocks.

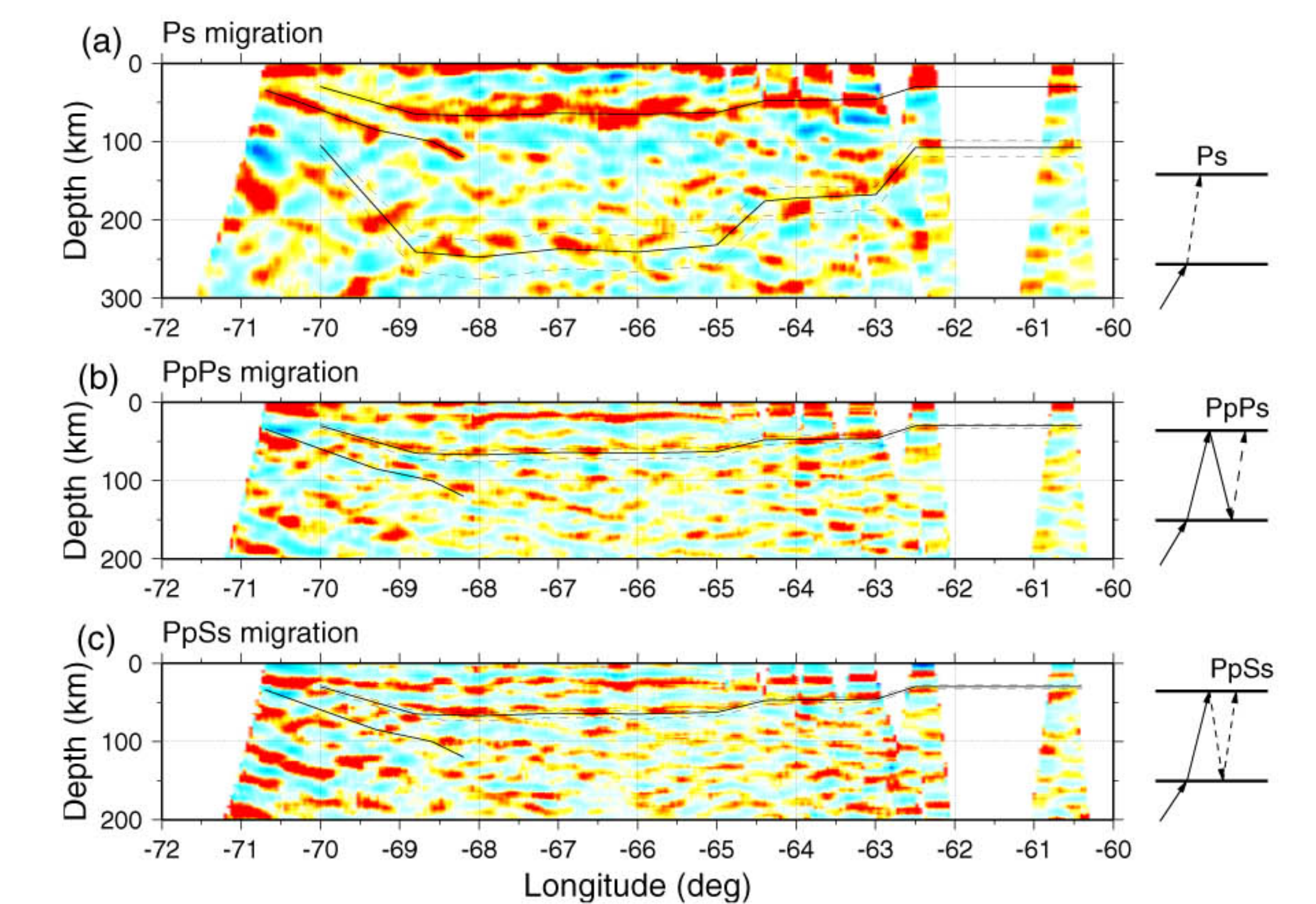


Fig. 6: Migrations of directly converted phase Ps (a) and two multiple phases PpPs (b) and PpSs (c) show that the continental Moho is clearly imaged by all three phases, and the average  $V_p/V_s$  ratio in the crust under the plateau is about 1.80 rather than 1.73. (a) is the upper 300 km part of Fig. 3. The amplitudes in (c) have been reversed after the PpSs migration. In the migration a  $V_p/V_s$  ratio of 1.73 is assumed. In the upper part of (a) the continental Moho and the subducted oceanic Moho are marked by solid lines which are again superposed on (b) and (c), indicating the position of the expected Moho position with a crustal  $V_p/V_s$  of 1.73. The solid line in the lower part of (a) is the central position of the PpPs multiple phase calculated by assuming a  $V_p/V_s$  of 1.73 and a slowness of 6.4  $s^\circ$ . The dashed lines in all plots are calculated multiple positions for crustal average  $V_p/V_s=1.83$  (above) and 1.63 (below). Note that both the PpPs and the PpSs multiple energy is above the 1.73 line, indicating a relative high  $V_p/V_s$  ratio beneath the Aedean plateau.

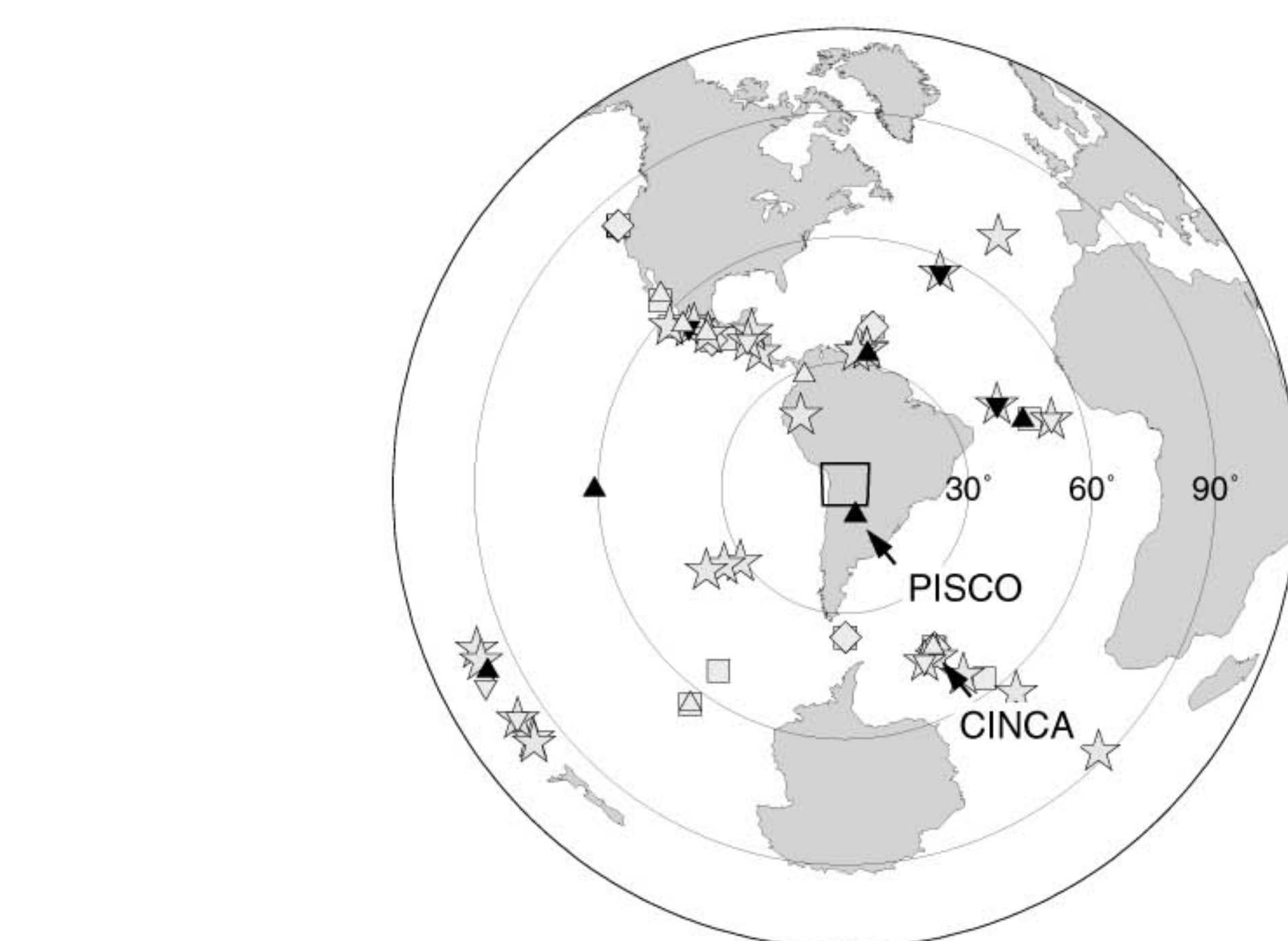


Fig. 2: Earthquakes recorded by different seismic arrays are shown with different symbols, which are identical with those in Fig. 1. Because of the global earthquake distribution pattern and the short observational periods, only a relatively small number of useful earthquakes within the epicentral distance range of 30°–95° have been recorded. Following data have been included in this study: two teleseismic earthquakes and two deep Argentinian earthquakes recorded by PISCO; six teleseismic earthquakes recorded by CINCA; three teleseismic earthquakes recorded by ANCORP; six teleseismic earthquakes recorded by PUNA. In addition to these networks, 5 broadband KDS stations have been operating for more than one year providing useful teleseismic data from more than 20 earthquakes. Data of the PASCALL broadband arrays BANJO and SEDA, operating from 1994 to 1995 have also been used.